 doi:10.20944/preprints202210.0139.v1

Article

Prediction of Dam Deformation Using SSA-LSTM Model Based on Empirical Mode Decomposition Method and Wavelet Threshold Noise Reduction

Caiyi Zhang [1],Shuyan Fu [1], Bin Ou [1,*],Zhenyu Liu [1] and Mengfan Hu

[1] College of Water Conservancy, Yunnan Agricultural University, Kunming 650201, China
* Correspondence: oubin418@126.com, oubin@ynau.edu.cn

Abstract: The deformation monitoring information of concrete dams contains some high-frequency components, and the high-frequency components are strongly nonlinear, which reduces the accuracy of dam deformation prediction. In order to solve such problems, this paper proposes a concrete dam deformation monitoring model based on empirical mode decomposition (EMD) combined with wavelet threshold noise reduction and sparrow search algorithm (SSA) optimization of long short-term memory network (LSTM). The model uses EMD combined with wavelet threshold to decompose and denoise the measured deformation data. On this basis, the LSTM model based on SSA optimization is used to mine the nonlinear function relationship between the reconstructed monitoring data and various influencing factors. The example analysis shows that the model has good calculation speed, fitting and prediction accuracy and it can effectively mine the date characteristics inherent in the measured deformation, and reduce the influence of noise components on the modeling accuracy.

Keywords: concrete dams; prediction model; empirical modal decomposition method; wavelet threshold; sparrow search algorithm; long short-term memory

1. Introduction

China is a large country of water conservancy construction, the number and scale of existing dams in the world's leading. To ensure the safe operation of dams is of great significance to maintain the safety of life and property of the public and regional stability. Deformation is an important monitoring quantity that reflects the comprehensive safety state of a dam. The construction of a high-precision deformation monitoring model can represent the evolution of the structural properties of a dam, quantitatively interpret the role of the main influencing factors and predict the operation of the dam, and evaluate the dam properties accordingly[1-3].

The dam deformation monitoring model can be divided into statistical model, deterministic model and hybrid models depending on the modeling approach[4, 5]. Because statistical models are easy to implement, they are widely used.With the development of computer technology such as gray theory[5, 6], neural network model[7-9], support vector machine model[10-12], random forest theory[13, 14] and many other methods are widely used in dam deformation monitoring model, which greatly improves the calculation speed and prediction accuracy of the monitoring model.However, these models have certain shortcomings. The random forest model has uncertainty in the empirical selection of parameters and runs relatively slowly, which can lead to situations such as poor classification in small data processing[15]. While neural network models are prone to overfitting and local optima when running. SVM models are suitable for problems such as small samples and nonlinearities, but the prediction performance of SVM models is strongly influenced by the selection of kernel parameters[16]. In order to make up for the shortcomings of these models, relevant personnel have proposed deep learning methods (such as

Preprints (www.preprints.org) | NOT PEER-REVIEWED | Posted: 11 October 2022 doi:10.20944/preprints202210.0139.v1

CNN[17], RNN[18], DBN[19]) and applied them to dam deformation monitoring. By studying the intrinsic laws and representation levels of monitoring data, the model can improve the prediction accuracy of complex nonlinear problems to a certain extent. Among them, the recurrent neural network is one of the more commonly used deep learning methods. The recurrent neural network (RNN) is designed based on the recursive nature of sequence data and is a feedback type of neural network. However, due to the disappearance of the gradient of RNN, the time series cannot exist for too long, so it can only have short-term memory and cannot support long-term memory, so the relevant personnel proposed the long short-term memory network (LSTM)[20, 21].

Long Short-Term Memory Networks (LSTMs) are derivatives that solve the problem of RNN gradient decay. The LSTM network combines short-term and long-term memory with gating, which solves the gradient decay problem to a certain extent. Ou Bin et al. [22]proposed a concrete dam deformation prediction model based on LSTM and verified that the model has good prediction accuracy and iteration rate in practical engineering. Wang et al.[23] proposed a prediction model combining ALO-LSTM and characteristic attention mechanism based on the existing earth dam seepage pressure prediction model, and quantitatively analyzed the degree of influence of each influence factor in the seepage pressure effect quantity. Dasan Yang et al [24] proposed an attention mechanism-based LSTM concrete dam deformation prediction method with Adma optimization algorithm to improve the learning accuracy and speed of LSTM, and verified the feasibility of the model in practical engineering. Liu et al [25]proposed a coupled long-term displacement prediction model for arch dams based on long and short memory networks. Principal component analysis (PCA) and moving average (MA) methods were used to reduce the dimensionality of the input variables,which are combined with LSTM to realize two coupled prediction models, LSTM-PCA and LSTM-MA, respectively. Affected by the measurement accuracy of the instrument and the inherent noise associated with the information acquisition module of the monitoring system, it is inevitable that there are certain random errors in the monitoring data that cannot be explained by environmental factors. In order to maximally eliminate the interference of unfavorable factors such as inherent noise and random errors, wavelet analysis[26, 27], singular value decomposition[28], variational mode decomposition (VMD)[29, 30], empirical mode decomposition (EMD)[31, 32] etc have been applied to the noise reduction of dam deformation monitoring data.

In view of the adverse effect of noise components in the measured deformation data on the modeling accuracy, this paper proposes a signal denoising method that combines empirical mode decomposition (EMD) and wavelet threshold method to decompose and reconstruct the data to make the unstable dam The monitoring data is stabilized to reduce the influence of noise in the measured deformation. In addition, in order to avoid local optima when the model algorithm performs deformation prediction, the Sparrow Search Algorithm (SSA) is used to optimize long and short -term memory networks (LSTM), Perform parameter optimization, and a concrete dam deformation prediction model based on the Sparrow search algorithm optimized LSTM is constructed. And applied to a certain engineering practice, the prediction accuracy and calculation speed of the model were analyzed and compared.

2. Selection of statistical models for dam deformation prediction

Dam deformation is the displacement vector sum of the plastic and elastic deformation of the concrete dam and bedrock under load. The displacement vector generated in the dam body can be decomposed into water pressure component δ_H , temperature component δ_T and time-dependent component δ_θ

$$\delta=\delta_H+\delta_T+\delta_\theta \tag{1}$$

The factor selection of the water pressure component δ_H , for the reason that the load of water pressure p_c is non-linear change. But the p_c with a curvilinear relationship of H , from which it can deduced that there is a relationship between δ_H and H , which is liner with H, H^2, H^3, H^4 . Besides, the δ_{2H} and δ_{2H} have the same relationship.

Preprints (www.preprints.org) | NOT PEER-REVIEWED | Posted: 11 October 2022 doi:10.20944/preprints202210.0139.v1

$$\delta_H = \sum_{i=1}^{4} a_{1i} H^i \tag{2}$$

Where a_i is structure coefficient; H is water depth value before the dam

According to analysis of the dam deformation monitoring data, temperature is one of the main factors affecting the arch dam.After years of normal operation of concrete dam, the hydration heat of the pour concrete has been completely dispersed,and the temperature inside the dam has reached a quasi-stable temperature field.At this time, the dam temperature is only influenced by the boundary temperature.Assume that water temperature and air temperature are harmonic motion, deformation and concrete temperature are linear relationship. Therefore, multi-period harmonics are chosen as the factor:

$$\delta_T(t) = \sum_{i=1}^{m_3} \left(b_{1i} \sin \frac{2\pi i t}{365} + b_{2i} \cos \frac{2\pi i t}{365} \right) \tag{3}$$

Where m_3 is 1 or 2, i is the annual cycle, t is the cumulative monitoring days.

Time-dependent component δ_θ, which general variation law of mathematical e xpression is a functional relationship when arch dam is normal operation. For concrete arch dams, it can be considered that the main factor of influencing the time-displacement is the viscous flow of the dam concrete and the dam base rock. The linear combination of θ and $\ln\theta$ can better describe the time-displacement caused by the rheological properties of the arch dam materials.

$$\delta_\theta = c_1\theta + c_2 \ln\theta \tag{4}$$

In summary, the time-varying forecast model for arch dam deformation can be expressed as

$$\begin{aligned} \delta &= \delta_H(t) + \delta_T(t) + \delta_\theta(t) \\ &= \sum_{i=1}^{4} a_{1i} H^i + \sum_{i=1}^{m_3} \left(b_{1i} \sin \frac{2\pi i t}{365} + b_{2i} \cos \frac{2\pi i t}{365} \right) + c_1\theta + c_2 \ln\theta \end{aligned} \tag{5}$$

3. Wavelet threshold-EMD based data noise reduction method

3.1. Empirical Mode Decomposition

Empirical Modal Decomposition Method, this is a noise reduction method for nonlinear and non-stationary data[33]. This method does not require manual setting of parameters, The original data can be quickly decomposed into high-to-low modal components, namely Intrinsic Mode Functions (IMF) and Residual (Res)[34], The specific decomposition and reconstruction steps are as follows:

For a given data sequence $x(t)$, Select the extreme value points in the data, And use the cubic spline difference function to form the upper and lower envelopes for the maximum point and the minimum point. Calculate the mean value of the upper and lower envelopes $m_1(t)$, subtract $m_1(t)$ from $x(t)$, Get a new time series denoted as $h_1(t)$

$$h_1(t) = x(t) - m_1(t) \tag{6}$$

However, it is difficult to solve the upper and lower package routes in reality, so it is necessary to use the spline difference function for fitting, and new extreme points will be generated during the fitting process. So it needs to go through the screening cycle until a certain stopping criterion is reached to end. That is, take $h_1(t)$ as a new $x(t)$ and loop the above operation k times to get $h_{1k}(t)$. which is:

$$h_{1k}(t) = h_{1(k-1)}(t) - m_1(t) \tag{7}$$

Where $h_{1(k-1)}(t)$ is the screening result of $k-1$ times, at this time h_{1k} is the first IMF component, denoted as $c_1(t)$

$$c_1(t) = h_{1k}(t) \tag{8}$$

Subtract $c_1(t)$ from given data $x(t)$ to get residual $r_1(t)$

Preprints (www.preprints.org) | NOT PEER-REVIEWED | Posted: 11 October 2022 doi:10.20944/preprints202210.0139.v1

$$r_1(t) = x(t) - c_1(t) \tag{9}$$

Continue to repeat the above steps until the residual is less than the preset error, or the residual is monotonic, At this point the EMD decomposition ends. which is:

$$x(t) = \sum_{i=1}^{n} c_i(t) + r_n(t) \tag{10}$$

In order to make the frequency and amplitude of the components obtained from the decomposition have a certain practical significance, it can faithfully reflect the volatility characteristics of the original sequence. In the process of decomposition screening, the standard deviation sum of adjacent screening results is 0.3.That is, the *SD* equation is:

$$SD = \sum_{k=1}^{T} \frac{\left| h_{1(k-1)}(t) - h_{1k}(t) \right|^t}{h_{1(k-1)}^2(t)} \tag{11}$$

3.2. Wavelet Threshold Noise Reduction

The basic principle of wavelet threshold de-noising is that after the signal is transformed by wavelet, the corresponding wavelet coefficients will be generated, select the appropriate threshold value, keep the wavelet coefficients larger than the threshold value, and remove the wavelet coefficients smaller than the threshold value[35]. The basic steps are as follows :(1) Select a wavelet with the number of layers N for decomposition. (2) Thresholding the decomposition coefficients of each layer. (3) Wavelet reconstruction according to the wavelet coefficients after deactivation. The wavelet threshold affects the selection of key parameters for noise reduction. Selecting appropriate parameters will achieve a good noise reduction effect. The main influencing factors are as follows:

Decomposition layer : When wavelet decomposition is performed on the original data, the higher the number of decomposition layers, the better the noise reduction effect but the signal is more likely to be distorted. The best result is achieved when the number of layers is chosen to be 3.

Basic wavelet function: For real signals, the basic wavelet selection usually considers factors such as support length, symmetry, trailing moments, smoothness and similarity. For one-dimensional signals such as audoi signals, dB wavelets and symbol wavelets are usually selected.

Threshold: Threshold selection is more important for wavelet threshold noise reduction. Common threshold selection methods include unbiased risk estimation threshold, minimax threshold, fixed threshold and heuristic threshold. This paper uses a fixed threshold:

$$\lambda = \delta\sqrt{2\log N} \tag{12}$$

At present, the commonly used threshold functions mainly include hard threshold function and soft threshold function, and the two threshold functions have their own advantages and disadvantages. Although the hard threshold function can well preserve the edge characteristics of the signal, it will cause a certain degree of distortion in the process of signal processing. The soft threshold function to remove noise after the signal is much smoother. Therefore, the soft threshold function is used in this paper.

Soft threshold function

$$\hat{w}_{thr} = \begin{cases} \left[\operatorname{sgn}(w)\right]\left(|w| - thr\right) & |w| \geq thr \\ 0 & |w| < thr \end{cases} \tag{13}$$

Where w_{thr} is the wavelet coefficient after wavelet transformation; λ is the threshold value; $\hat{w}_{thr}$ c is the wavelet coefficient denoised by the threshold value.

Considering that the EMD method and the wavelet threshold method have their own advantages and disadvantages in data preprocessing, and the two methods can complement each other. For the high-frequency components decomposed by EMD, the wavelet threshold can be used for noise reduction, which effectively reduces the distortion of the

Preprints (www.preprints.org) | NOT PEER-REVIEWED | Posted: 11 October 2022 doi:10.20944/preprints202210.0139.v1

signal. Therefore, a noise reduction method based on EMD combined with wavelet threshold is constructed based on the above principles.

4.The prediction model based on optimized LSTM model with Sparrow search algorithm

4.1. Sparrow search algorithm

Jiankai xue[36] proposed a new intelligent optimization algorithm which is sparrow search algorithm (SSA) in 2020. This algorithm is mainly inspired by the foraging behavior of sparrows, has the characteristics of strong merit-seeking ability and fast convergence. The sparrow search algorithm avoids the algorithm falling into local optimum by constructing the corresponding fitness function, which makes the identity of individual sparrows, and the position change dynamically. In the simulation experiment, we need to use virtual sparrows for food hunting, and the population X consisting of n sparrows can be expressed in the following form:

$$X = \begin{bmatrix} x_{1,1} & x_{1,2} & \cdots & x_{1,d} \\ x_{2,1} & x_{2,2} & \cdots & x_{2,d} \\ \vdots & \vdots & \vdots & \vdots \\ x_{n,1} & x_{n,2} & \cdots & x_{n,d} \end{bmatrix} \tag{14}$$

Where d is the dimension of the sparrow population, n is the number of sparrows, x is the sparrow individual.

The fitness values of all sparrows can be expressed in the following form

$$F_X = \begin{bmatrix} f\left(\begin{bmatrix} x_{1,1} & x_{1,2} & \cdots & x_{1,d} \end{bmatrix}\right) \\ f\left(\begin{bmatrix} x_{2,1} & x_{2,2} & \cdots & x_{2,d} \end{bmatrix}\right) \\ \vdots \\ \vdots \\ f\left(\begin{bmatrix} x_{n,1} & x_{1n2} & \cdots & x_{n,d} \end{bmatrix}\right) \end{bmatrix} \tag{15}$$

Where F_X is the Adaptability matrix, f is the Adaptability value. Sparrows with better adaptability values (discoverers) will prefer to guide foraging direction and range when foraging in groups, due to the greater foraging range of discoverers.

During each iteration of the sparrow search algorithm, the location update of the discoverer is described as follows:

$$x_{i,j}^{t+1} = \begin{cases} x_{i,j}^{t} \exp\left(\dfrac{-i}{\alpha iter_{\max}}\right), R_2 < ST \\ x_{i,j}^{t} + QL, R_2 \geq ST \end{cases} \tag{16}$$

Where *iter* is the Current iteration factor; $iter_{\max}$ is the constant with the highest number of iterations; $x_{i,j}^{t}$ is the value of the j dimension of the i sparrow at the t iteration, $j = 1, 2, 3, \cdots, d$; $\alpha \in (0,1]$; $R_2 = [0,1]$ is the Alarm value; $ST \in [0.5,1]$ is the Safety threshold value, Q is the random numbers that obey the normal distribution; L is a $1 \times d$ order matrix.

When $R_2 < ST$, there is no danger around at this point, the discoverer can continue to search for food.

When $R_2 \geq ST$, there is danger around at this time, discoverer need to take cover to ensure safety quickly.

However, for sparrow populations,once the discoverer searches for a quality food source, the joiner will recognize it and fly near it to grab food during foraging. At the same time, some joiners will always watch the discoverer and ready to fight for food. Thus, the location update plan result from joiner as follows:

Preprints (www.preprints.org) | NOT PEER-REVIEWED | Posted: 11 October 2022 doi:10.20944/preprints202210.0139.v1

$$x_{i,j}^{t+1} = \begin{cases} Q\exp\left(\dfrac{X_{worst} - X_{i,j}^{t}}{i^2}\right), i > \dfrac{n}{2} \\ x_p^{t+1} + \left|x_{i,j}^{t} - x_p^{t+1}\right| A^{+} L, \text{other} \end{cases} \tag{17}$$

Where x_p is the Producer Optimal Location; x_{worst} is the Worst position; A is the $1 \times d$ order matrix and any element is randomly assigned a value of 1 or -1. When $i > \dfrac{n}{2}$, it indicates that the ith joiner failed to grab the food and needs to forage again for it.

In conclusion, assuming 10%-20% of sparrows aware of the danger, the initial position random generation rule is:

$$x_{i,j}^{t+1} = \begin{cases} x_{best}^{t} + \lambda\left|x_{i,j}^{t} - x_{best}^{t}\right|, f_i > f_g \\ x_{i,j}^{t} + k\dfrac{\left|x_{i,j}^{t} - x_{worst}^{t}\right|}{f_i - f_w + \varepsilon}, f_i = f_g \end{cases} \tag{18}$$

Where λ is the Step control function, obey a normal distribution with mean 0 and variance 1; f_i is the Current sparrow adaptation values; f_g is the Global optimal adaptation value; x_{best} is the Global best position; k is the Direction of movement; ε is the Minimum Constant. When $f_i > f_g$, Sparrows are more dangerous at the fringes of the population. When $f_i = f_g$, Aware of the danger, the sparrow moves closer to other sparrows for safety in order to avoid it.

4.2. LSTM Neural Networks

LSTM is a special form of the traditional recurrent neural network(RNN), which was proposed by Sepp Hochreiter in 1977 for the gradient vanishing problem of RNN. Compared with RNN, which has only one state h in the hidden layer, LSTM adds a unit state c to the original structure of RNN. In order to make long-term preservation of short-term input, LSTM proposes to store and update the cell state in the form of "gate". The concepts of input gate, forget gate and output gate are proposed, and the long-term retention of information is finally realized through the control of the three gates. As shown in Figures 1 and 2.

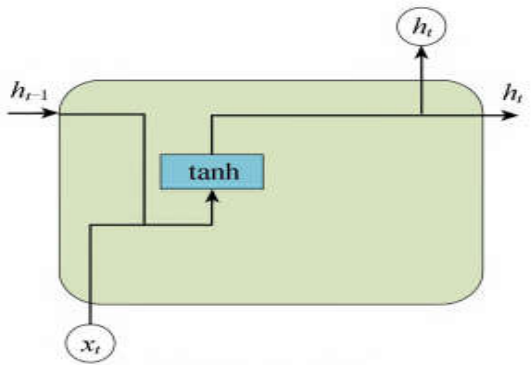

Figure 1. RNN cell structure .

Preprints (www.preprints.org) | NOT PEER-REVIEWED | Posted: 11 October 2022 doi:10.20944/preprints202210.0139.v1

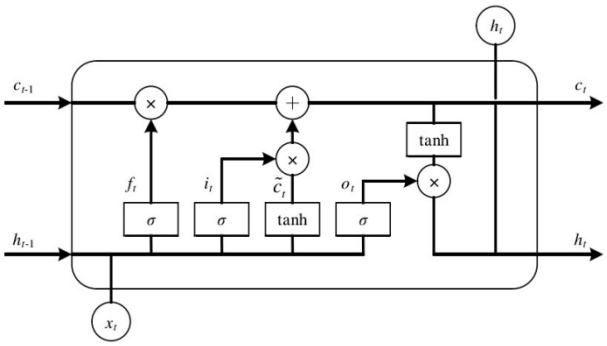

Figure 2. LSTM cell structure.

The forget gate controls the proportion of the unit state from the previous moment saved to the current moment. The formula *sigmoid* can be obtained by the activation function:

$$f_t = \delta\left(W_f \cdot [h_{t-1}, x_t) + b_f\right) \tag{19}$$

Where W_f is the Weight matrix of the forgotten gate; b_f is the Offset items; δ is the sigmiod Stimulus function; x_i is the Current input; h_{t-1} is the Hidden output in the previous moment.

The input gate controls the proportion of the network state saved to the cell state at the current moment. The following formula is

$$i_t = \delta\left(W_i \cdot [h_{t-1}, x_t) + b_i\right) \tag{20}$$

$$\tilde{C}_t = \tanh\left(W_c \cdot [h_{t-1}, x_t) + b_c\right) \tag{21}$$

Where W_i is the Weight matrix of the sigmoid layer; b_i is the Bias term for the input gate sigmoid layer; W_c is the Weight matrix of the input gate tanh layer; b_c is the Bias term for output gate tanh layer.

The expression after cell state update is:The expression after cell state update is

$$C_t = f_t C_{t-1} + i_t a_t \tag{22}$$

The output gate can extract valid information from the current cell state to be used in a new hidden layer. The mathematical expression of the output gate is:

$$o_t = \sigma\left(W_o \cdot [h_{t-1}, x_t) + b_o\right) \tag{23}$$

Where W_o is the Weight matrix of the output gate; b_o is the Bias term for the output gate.

Final output of LSTM:

$$h_t = o_t \tanh C_t \tag{24}$$

5. Construction of the model

Affected by the measurement accuracy of the instrument and the inherent noise associated with the information acquisition module of the monitoring system, it is inevitable that there are certain random errors in the monitoring data that cannot be explained by environmental factors, which will lead to prediction accuracy when building a dam deformation monitoring model. Therefore, it is necessary to perform prediction preprocessing on the data.In this paper, the combined noise reduction approach based on EMD combined with wavelet threshold is used to decompose and reconstruct the original data. and combined with the sparrow search algorithm (SSA) to optimize the LSTM model, a concrete dam deformation monitoring model based on empirical mode decomposition (EMD) combined with wavelet threshold noise reduction And combined with the sparrow search algorithm (SSA) to optimize the long short-term memory network (LSTM) was constructed. The specific process is shown in Figure 4 below:

Step1: The monitored raw data is decomposed by EMD, and the IMF components obtained from the decomposition are distributed from high to low. Perform wavelet

Preprints (www.preprints.org) | NOT PEER-REVIEWED | Posted: 11 October 2022 doi:10.20944/preprints202210.0139.v1

threshold noise reduction on high-frequency IMF components, reconstruct the high-frequency IMF components after noise reduction and low-frequency IMF components, and obtain the data after noise reduction;

Step2: Initialize and normalize the denoised data. Determine the following parameters: Length of LSTM time window, Number of hidden layer cells,Sparrow population size and The Number of iterations. Subsequently, initial Safety Threshold and Sparrow Position;

Step3: Use the predicted value of the LSTM algorithm and the root mean square of the sample data to determine the fitness value of each sparrow;

Step4: Update the sparrow position, get a new fitness value, and search for the optimal position of the population and the global optimal value;

Step5: Perform iterations, determine whether the maximum number of iterations is reached, and obtain the optimal individual solution. Stop the iteration if the maximum value is reached and determine the optimal parameters of the LSTM. if not, repeat the loop step;

Step6: Substitute the obtained LSTM parameters into the training grid to make predictions;

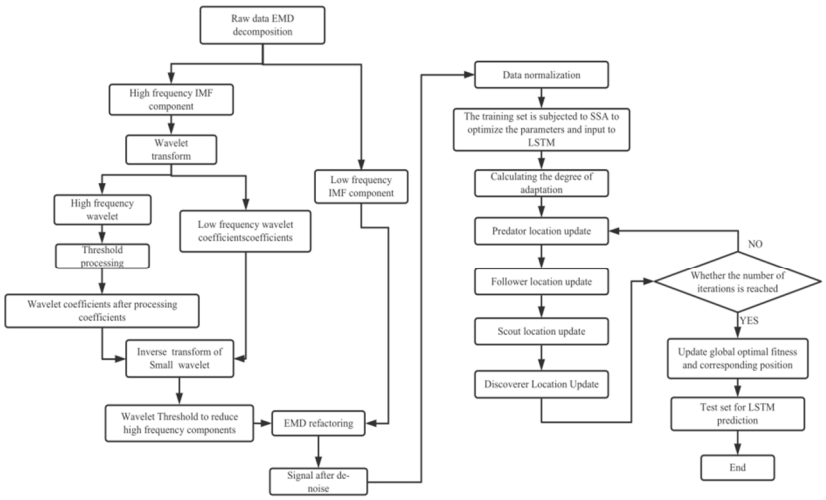

Figure 3. Concrete arch dam prediction process based on EMD combined with wavelet threshold noise reduction coupled with SSA-LSTM.

6. Construction of the model

6.1. Factsheet

A hydropower station is located in southwestern Yunnan Province. The dam is a concrete double-bend arch dam with a crest elevation of 1245m. The maximum dam height is 292m, the dam crest length is 992.74m, the arch crown beam top width is 13m, and the arch crown beam bottom width is 69.49m. Considering the low frequency of manual observation, measurement points were selected from the automatic measurement points for comparative analysis. Among them, C4-A22-PL-05 measurement points are highly reliable, with fewer missing or jumping data and fewer instrument failures, which can provide longer and more accurate deformation monitoring data. A point is selected at the dam body as an observation point, and the upstream and downstream water levels and temperatures corresponding to this measurement point are shown in Figure 4, Figure 5, and Figure 6 below.

Preprints (www.preprints.org) | NOT PEER-REVIEWED | Posted: 11 October 2022 doi:10.20944/preprints202210.0139.v1

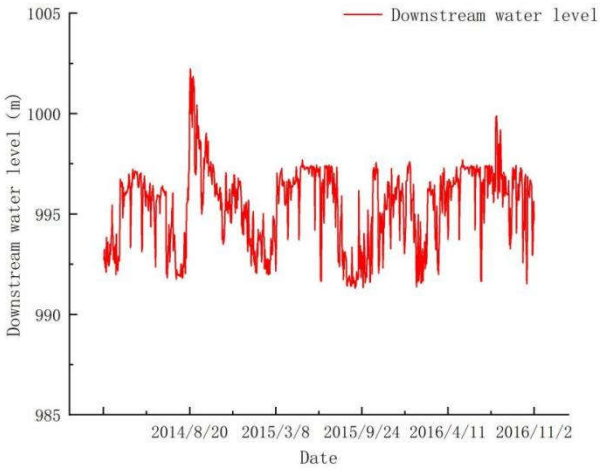

Figure 4. C4-A22-PL-05 measurement point downstream water level.

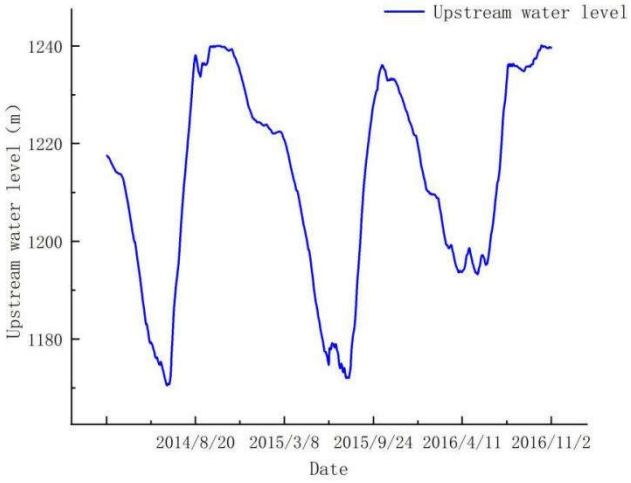

Figure 5. C4-A22-PL-05 measurement point upstream water level.

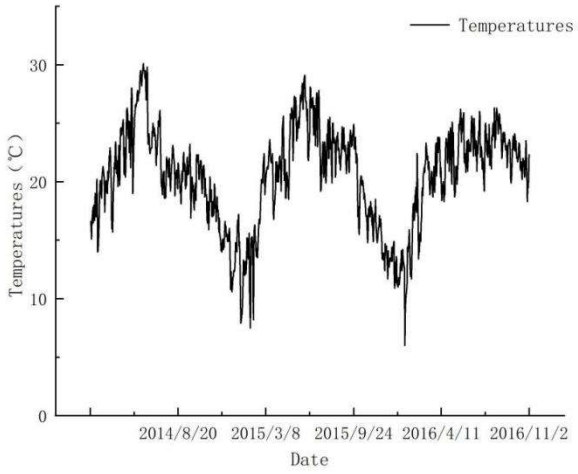

Figure 6. C4-A22-PL-05 measuring point air temperature.

Preprints (www.preprints.org) | NOT PEER-REVIEWED | Posted: 11 October 2022 doi:10.20944/preprints202210.0139.v1

6.2. Data Noise Reduction Based on EMD Combined with Wavelet Threshold

Since the wavelet threshold noise reduction in the data processing although the results a re smoother, but in the extreme points will still be more blurred, and the traditional EMD method will remove the high-frequency components, the use of low-frequency components for reconstruction in a certain degree will make the signal distortion. Therefore, this paper proposes a noise reduction method based on EMD combined with wavelet threshold. First, the original monitoring data of the dam is decomposed by EMD, the high-frequency IMF components obtained from the decomposition are denoised by the wavelet threshold, and the low-frequency components obtained by the EMD decomposition are reconstructed. This method effectively avoids the signal distortion caused to some extent by the traditional EMD method. In this paper, different methods are used to denoise the data. The analysis results and the IMF components are shown in Figures 7 below:

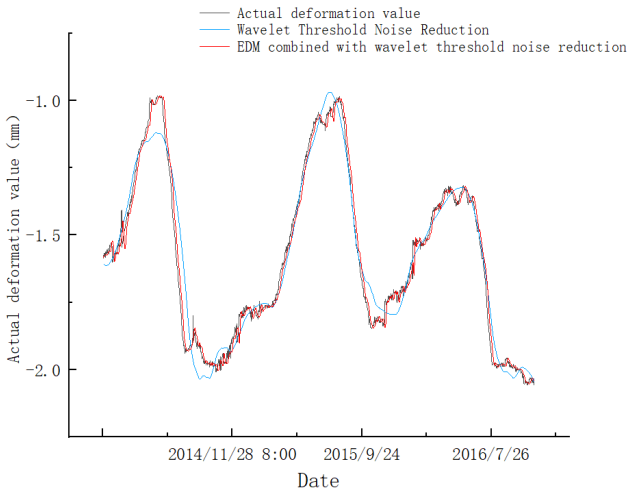

Figure 7. C4-A22-PL-05 noise reduction comparison of measurement points.

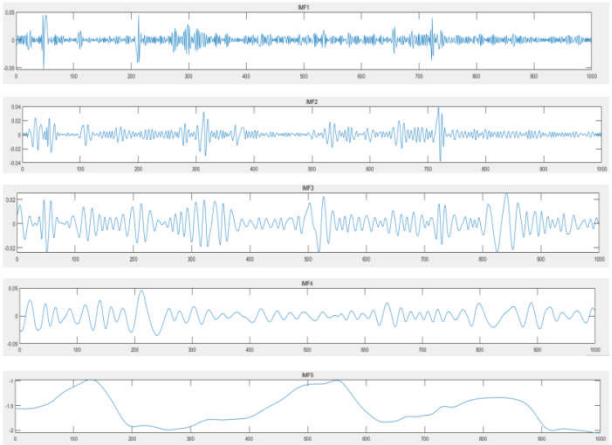

Figure 8. IMF components after noise reduction based on EMD combined with wavelet thresholds.

It can be seen from Figures 7 and 8 that after the dam deformation signal is processed based on EMD combined with the wavelet threshold noise reduction method, it is decomposed into five components, which are arranged in order from top to bottom by frequency. Using EMD combined with wavelet threshold noise reduction, the burrs near the extreme points are significantly reduced, the data at the peaks and valleys are smoother, and the amplitude of the signals at the peaks and valleys is well preserved. Compared with the wavelet threshold noise reduction effect, the denoising effect is very ideal, and can well maintain the basic shape of the original data of the dam deformation.

Preprints (www.preprints.org) | NOT PEER-REVIEWED | Posted: 11 October 2022 doi:10.20944/preprints202210.0139.v1

6.3. Model analysis

As there are many factors affecting the deformation of arch dams, such as the time factor, the water pressure factor and the temperature. Therefore the choice of model parameters is more important. For the model input 10 vectors, where the timing factor is a combination of linear θ and $\ln\theta$, taken $(\theta-\theta_0)$、$(\ln\theta-\ln\theta_0)$、The temperature factor is taken $\sin\frac{2\pi t}{365}-\sin\frac{2\pi t_0}{365}$、$\cos\frac{2\pi t}{365}-\cos\frac{2\pi t_0}{365}$、$\sin\frac{4\pi t}{365}-\sin\frac{4\pi t_0}{365}$、$\cos\frac{4\pi t}{365}-\cos\frac{4\pi t_0}{365}$ Since the dam is a concrete hyperbolic arch dam therefore the water pressure factor is taken as $(H-H_0)$、$(H-H_0)^2$、$(H-H_0)^3$、$(H-H_0)^4$. After selecting the impact factor and the effect dose, in order to eliminate the influence of the dimension and the magnitude difference between the impact factor is too large, the impact factor and the effect dose are normalized. The nodes of the input layer and output layer of the LSTM model in this paper are 1 and 9 respectively, the number of units in the two LSTM hidden layers is 100 and 50 respectively, and the maximum number of iterations is set to 40 and 320 respectively. Select the training set and test set, use the training set data to make the model fully learn the deformation law of the dam, and use the trained prediction model to predict the deformation of the prediction set data.

In this paper, the monitoring data of measurement point C4-A22-PL-05 from February 2, 2014 to June 16, 2015 were selected for parameter searching optimization of SSA-LSTM. Sparrow population is 10, iteration number is 50, search dimension is 4, learning rate range $[0.001, 0.01]$. The dam deformation data from the C4-A22-PL-05 measuring point from June 17, 2015 to April 13, 2016 are used as the training set, and the dam monitoring data from April 13, 2016 to November 2016 are used as the test set, carry out testing. In order to verify the validity of the model, different models LSTM, SVM and PSO-SVM are used to construct the corresponding prediction models. The prediction results of the four models are shown in table 1, The prediction curves and model residuals are shown in figures 9 and 10 below :

Table 1. Prediction results of each prediction model.

Measuring points	Predictive Models	RMSE/mm	MAE/mm²	R^2
C4-A22-PL-05	SSA-LSTM	0.0163	0.00846	0.9987
	LSTM	0.0913	0.07611	0.9036
	PSO-SVM	0.1293	0.09564	0.8852
	SVM	0.06358	0.05345	0.9533

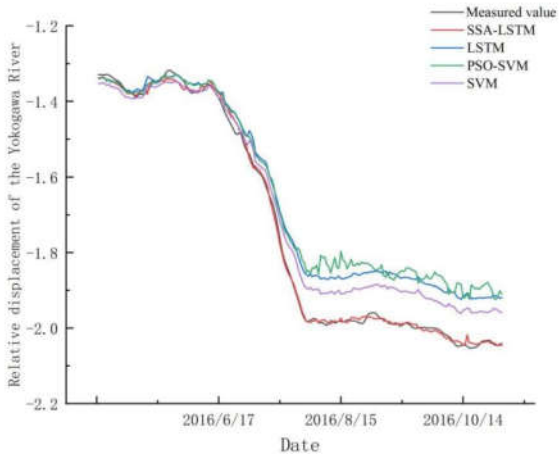

Figure 9. C4-A22-PL-05 measurement point prediction curve.

Preprints (www.preprints.org) | NOT PEER-REVIEWED | Posted: 11 October 2022 doi:10.20944/preprints202210.0139.v1

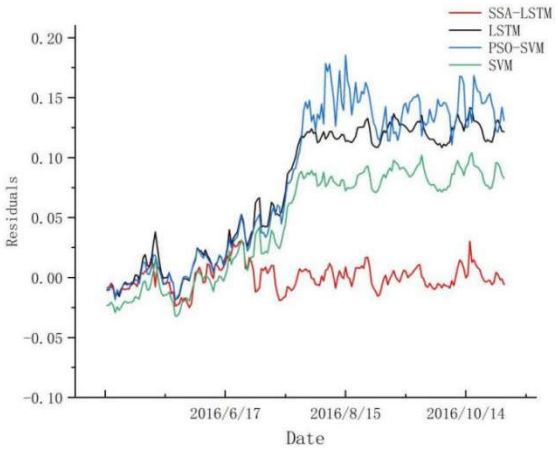

Figure 10. C4-A22-PL-05 measurement point prediction residuals.

According to the cross-river displacement prediction curve and residual of C4-A22-PL-05 measuring point in Figs 9-10, it can be seen that the prediction model constructed by SSA-LSTM, LSTM, SVM and PSO-SVM is generally consistent with the actual displacement change process. In comparison, the prediction model of SSA-LSTM algorithm is closer to the measured deformation than the prediction results of LSTM, SVM and PSO-SVM prediction models. At the same time, the model residual has no obvious change rule and its change range is significantly smaller. The SSA-LSTM model fits better than the other three models, and its residual variation range fluctuates less, indicating that the model can more accurately represent the complex nonlinear functional relationship between the impact factor and the dam deformation. The correlation results in Table 1 show that the SSA-LSTM model predicts the segment MAE, MSE are smaller, and the complex correlation coefficient R2 is closer to 1 compared with the remaining three models, which further verifies the good prediction performance of the model.

7. Conclusion

1. This paper proposes a noise reduction method based on EMD combined with wavelet threshold, using the EDM method to decompose the original monitoring data of the dam, and applying wavelet threshold noise reduction to the decomposed high frequency IMF components. The high-frequency IMF components after noise reduction are obtained, and the low-frequency IMF components obtained by decomposition are combined for reconstruction. A prediction model is constructed from the denoised data, which improves the prediction accuracy of the SAA-LSTM model.

2. This paper uses the sparrow search algorithm to optimize the long short-term memory (LSTM), and uses the good stability, convergence speed, scalability and robustness of the sparrow search algorithm to perform grid training and parameter optimization of the LSTM. The global optimal location and fitness values are updated, and the optimized LSTM model is optimized in terms of the number of hidden layer nodes and learning rate using grid search to effectively mine the complex functional relationship between the dam deformation and its influence factors.

3. The three deformation prediction models of LSVM, SVM and PSO-SVM are compared by using the example verification analysis. Compared with the other three models, the prediction accuracy and convergence speed of the SSA-LSTM model have been significantly improved, providing a new method for predicting dam deformation with high accuracy, which is more suitable for actual engineering situations.

Author Contributions:Conceptualization,,Z.C,B.O.validation,S.F,Z.L.andM.H.;writing-oniginal draft preparation, C.Z.;methodology ,C.Z.;funding,B.O,S.F.;All authors have read and agreed to the published version of the manuscript.

Funding: The work is supported by National Natural Science Foundation of China [No. 52069029].

Data Availability Statement: Original date is available upon reasonable requests.

Conflicts of Interest: The authorsdeclare no conflict of interest.

References

[1] Wei.W.;Lou.S.Y.;Xu.F.A combined displacement prediction model for concrete arch dams based on monitoring time-series decomposition and reconfiguration. *Engineering Science and Technology*.**2022**: 1-13.doi:10.15961/j.jsuese.202100544.

[2] Li.Y.; Bao.T.;Shu.X. A Hybrid Model Integrating Principal Component Analysis, Fuzzy C-Means, and Gaussian Process Regression for Dam Deformation Prediction. *Arabian journal for science and engineering*.**2021**(46-5).doi:10.1007/s13369-020-04923-7

[3] Kang.F.;Liu.J.;Li.J. Concrete dam deformation prediction model for health monitoring based on extreme learning machine. *Structural Control and Health Monitoring*.**2017**,24(10).doi:10.1002/stc.1997

[4] Fan.Z.D.;Cui.W.J.;Chen.M. IPSO-RVM based dam safety warning model. *Journal of Changjiang Academy of Sciences*. **2016**,33(02): 48-51.doi:10.11988/ckyyb.20140801

[5] Huang.W.Y.;Fan.Z.C. Application of Gray Self-Memory Model in Prediction of Ice Flood Water Level of the Yellow River. *Yellow River*, **2013**.

[6] Yang.S.H.;Chen.T. Research on electrical main wiring fault monitoring model for water conservancy projects based on grey system theory. *Hydropower Technology*. **2020**,51(10): 88-95.doi:10.13928/j.cnki.wrahe.2020.10.011

[7] Lin.Z.Y. Research on Deformation Prediction Model of Earth-rock Dam Based on BP Neural Network. *People's Pearl River*. **2020**,41(06): 74-78.doi:CNKI:SUN:RMZJ.0.2020-06-014

[8] Chen.Z.A.;Xiong.X.;You.Y.Y. Variational modal decomposition and long-short time neural networks for dam deformation prediction. *Mapping Science*.**2021**,46(09): 34-42.doi:10.16251/j.cnki.1009-2307.2021.09.004.

[9] Shao.N.;Yu.Z.W. Application of wavelet neural networks in dam deformation forecasting. *Urban Surveys.* **2018**(04): 156-157.doi:CNKI:SUN:CSKC.0.2018-04-043

[10] Wei.B.W.;Liu.B.;Xu.F.G. Hybrid model for multi-measurement point deformation monitoring of concrete arch dams incorporating PSO-SVM. *Journal of Wuhan University (Information Science Edition)*.**2021**: 1-14.doi:http://kns.cnki.net/kcms/detail/42.1676.TN.20211028.1238.010.html

[11] Huai.Z.S.;Zhe.X.C.;Zhi.P.W. Performance improvement method of support vector machine-based model monitoring dam safety. *Structural Control & Health Monitoring*.**2016**,23(2): 252-266.doi:10.1002/stc.1767

[12] Li.M.;Pan.J.;Liui.Y. A Deformation Prediction Model of High Arch Dams in the Initial Operation Period Based on PSR-SVM-IGWO. *Mathematical Problems in Engineering.* **2021**.doi:10.1155/2021/8487997

[13] Luo.H.;Guo.S.Y.;Bao.W.M. Random Forest Model and Application for Arch Dam Deformation Monitoring and Prediction. *South-to-North Water Diversion and Water Conservancy Technology*. **2016**,14(06): 116-121.doi:10.13476/j.cnki.nsbdqk.2016.06.020.

[14] Li.X.;Wen.Z.;Su.H. An approach using random forest intelligent algorithm to construct a monitoring model for dam safety. *Engineering With Computers*. **2019**(3).doi:10.1007/s00366-019-00806-0

[15] Yi.Z.Y.;Su.H.Z.;Yang.L.F. Combined modeling method of random forest and swordfish optimization for deformation monitoring model of concrete dam. *Hydropower and Energy Science*. **2021**,39(10): 106-109.

[16] Wei.B.W.;Yuan.D.Y.;Bin.X. Deformation prediction model of concrete dam based on optimal correlation vector machine based on chicken swarm algorithm. *Water Conservancy and Hydropower Technology*. **2020**,51(04): 98-105.doi:10.13928/j.cnki.wrahe.2020.04.011.

[17] Zhi.P.;Zen.G.;Hai.D. Self CNN-based time series stream forecasting. *Electronics Letters.* **2016**,52(22): 1857-1858.doi:10.1049/el.2016.2626

[18] Min.K.;Ki.M.D.;Pa.R.;K.J. RNN-Based Path Prediction of Obstacle Vehicles With Deep Ensemble. I*EEE Transactions on Vehicular Technology*. **2019**,PP(99): 1.doi:10.1109/TVT.2019.2933232

[19] Hu.C.H.;Pei.H.;Si.X.S. A Prognostic Model Based on DBN and Diffusion Process for Degrading Bearing. *IEEE Transactions on Industrial Electronics.* **2019**,PP(99): 1.doi:10.1109/TIE.2019.2947839

[20] Li.Y.;Bao.T.;Gong. The prediction of dam displacement time series using STL, extra-trees, and stacked LSTM neural network. *IEEE Access*. **2020**,PP(99): 1.doi:10.1109/ACCESS.2020.2995592

[21] Zhang.J.;Cao.X.;Xie.J. An Improved Long Short-Term Memory Model for Dam Displacement Prediction. *Mathematical Problems in Engineering*. **2019**,2019(1): 1-14.doi:10.1155/2019/6792189

[22] Ou.B,Wu.B.B.;Yuan.J. Deformation prediction model of concrete dam based on LSTM. *Progress in Water Conservancy and Hydropower Science and Technology*. **2022**,42(01): 21-26.doi:10.3880/j.issn.10067647.2022.01.003

[23] Wang.X.L.;Li.K.;Zhang.Z. Seepage pressure prediction model of earth-rock dam coupled with ALO-LSTM and feature attention mechanism. *Journal of Hydraulic Engineering*. **2022**,53(04): 403-412.doi:j.cnki.slxb.20210936.

[24] Yang.D.S,.;Gu.C.S.;Zhu.Y.T. A Concrete Dam Deformation Prediction Method Based on LSTM With Attention Mechanism.. *IEEE Access*. **2020**,8: 185177-185186.doi:10.1109/access.2020.3029562.

[25] W.L.;J.P.;Y.R. Coupling prediction model for long-term displacements of arch dams based on long short-term memory network. *Struct Control Health Monit*. **2020**: e2548.doi:10.1002/stc.2548

[26] Luo.D.H.;J.Z.D. Wavelet analysis and ARMA prediction model for dam deformation. *Journal of Water Resources and Water Transport Engineering*. **2016**(03): 70-75doi:10.16198/j.cnki.1009-640X.2016.03.009.

[27] Huai.Z.;Xing Y. Wavelet support vector machine-based prediction model of dam deformation. *Mechanical Systems & Signal Processing*. **2018**(110-).

[28] Yang.G.;Fan.Z.D.;Fu.C.J. Research on outlier identification techniques for dam safety monitoring data based on singular spectrum analysis. *Hydroelectricity*. **2021**,47(08): 125-129.doi:10.3969/j.issn.0559-9342.2021.08.024

[29] Zhang.J.F.;Heng.Y. Concrete dam deformation prediction model based on VMD-PE-CNN. *Hydropower Technology (English and Chinese)*. **2022**: 1-11.doi:http://kns.cnki.net/kcms/detail/10.1746.TV.20220805.1519.010.html

[30] Hu.H.;Zhang.J.; Li.T. A Novel Hybrid Decompose-Ensemble Strategy with a VMD-BPNN Approach for Daily Streamflow Estimating. Water Resources Management: An International Journal, *Published for the European Water Resources Association (EWRA)*. **2021**,35.doi:10.1007/s11269-021-02990-5

[31] Liu.S.M.;Xu.J.T.;Ju.B.X. Dam deformation prediction based on EMD and RBF neural networks. *Mapping Bulletin*. **2019**(08): 88-91.doi:10.13474/j.cnki.11-2246.2019.0258.

[32] Chen.Y. Back analysis of permeability coefficient of earth-rock dam based on EMD-RVM. *IOP Conference Series Earth and Environmental Science*. **2020**,560: 12095.doi:10.1088/1755-1315/560/1/012095

[33] Sheng.J.J.;TengF.B.;D.H.C. Dam deformation prediction model and application based on EMD decomposition method. *Water Conservancy and Hydropower Technology*. **2017**,48(12): 41-44.doi:10.13928/j.cnki.wrahe.2017.12.007

[34] Xu.X.Y.;Zhang.P.F.;Jian.J. Research on dam deformation prediction based on EMD-PSO-ELM algorithm. *Software Guide*. **2020**,19(09): 1-5.doi:CNKI:SUN:RJDK.0.2020-09-002

[35] Xin.D.L.;Huan.Y.C.;Cai.Q.S. Ultra-short-term wind power prediction based on wavelet threshold noise reduction and BP neural network. *World Science and Technology Research and Developmen*t. **2011**,33(06): 1006-1010.doi:10.16507/j.issn.1006-6055.2011.06.018

[36] Xue.J.K. Research and application of a novel swarm intelligence optimization technique. Donghua University. 2020.doi:10.27012/d.cnki.gdhuu.2020.000178.